Statistics of bursts in the solar corona at X-ray wavelength

A thesis submitted towards partial fulfilment of
BS-MS Dual Degree Programme

by

Shashwat Antony

under the guidance of

Dr. Prasad Subramanian

AFFILIATION OF THE SUPERVISOR

Indian Institute of Science Education and Research
Pune

Certificate

This is to certify that this thesis entitled "Statistics of bursts in the solar corona at X-ray wavelength" submitted towards the partial fulfilment of the BS-MS dual degree programme at the Indian Institute of Science Education and Research Pune represents original research carried out by "Shashwat Antony" at "Indian Institute Of Science Education And Research, Pune", under the supervision of "Dr Prasad Subramanian" during the academic year 2013-2014.

Student
Shashwat
Antony

Supervisor
Dr. Prasad
Subramanian

Acknowledgements

I express my deepest gratitude to my supervisors Dr.Prasad Subramanian and Dr. M. S. Santhanam for giving me the opportunity to work on this project and for their continuous guidance, advice and moral support.

I am indebted to my friends Danveer Singh, Neelesh Soni and Abhijit Awadhiya for encouraging me throughout this final year. Words cannot express my gratitude to my family for their blessings and support without which it would not have been possible to complete this thesis.

Abstract

It was discovered during the working of early radars that solar radiation interferes with terrestrial radio signals. There have been studies to prove this interference. In this study our goal was to quantify this interference through the signal to noise ratio. We analysed the X-ray radiation flux and reaffirmed the existence of power law in the flux. We studied the solar flares of different classes through waiting-times. We conducted fluctuation analysis for the flux and for subsequent first differences of the flux and found the existence of power law at multiple levels. We used DFA to determine the strength of correlation in our X-ray data set and found that X-ray radiation flux pertains to 1/f noise pattern.

Contents

1 Introduction **3**
1.1 Solar Flare 3
1.2 Data Sources 3

2 Study of underlying Distributions of data **5**
2.1 Power law index 5
2.2 Waiting Time Distribution 8

3 First difference of the time series **11**
3.1 Frequency Distribution of first differences 11
3.1.1 Note on frequency distribution of First differences . . . 14
3.1.2 Note on Power law index of of First differences 15

4 Fluctuation analysis **19**
4.1 DFA 19
4.1.1 Note on DFA exponents 20

5 Discussion **23**

References **24**

Chapter 1

Introduction

In this study we have used solar radiation flux data to analyse the radiation output of the sun as a whole and on different classes of Solar flares.

1.1 Solar Flare

Solar flare is a phenomena in which sun releases large amount of energy from its surface. Sun contains large number of magnetic domains of different sizes on its surface. When a magnetic domain is reconfigured or becomes unstable the energy stored in the domain(field maintained by the domain) is released. This causes a burst in radiation along with release of charged particles which appears as an arc coming out of the sun. The region where this event occurs on the surface of the sun is called a sunspot. This event is observed by recording the radiation flux and imaging of the sun. In this study we are focusing on radiation flux. Solar flare are classified into 5 classes in increasing order of magnitude: A,B,C,M and X. Each class is further divided into subclasses.

1.2 Data Sources

The data sources can be categorised into two categories: high frequency and low frequency observations. For radiation corresponding to X-ray region of spectrum the atmospheric scattering prevents any observation on ground level. This problem is not there for radiation corresponding to visible and above(increasing wavelength). For our study we obtained X-ray flux data from NOAA database[7]. This data was recorded by GOES satellite series (GOES 05 to GOES 12) from 1986 to 2010. There are two channels present for X-ray observation: long channel(1 to 8 Angstroms) and short channel(0.5

to 4 Angstroms). We used only the long channel for our study. The threshold flux for long channel is 2x10$^{-8}W/m^2$ and short channel is 5x10$^{-9}W/m^2$[8]. So for the first differences set we have replaced the zeroes it with 1% of threshold value for convenience and to account for sensitivity of the sensors. The data is provided for time intervals of 3 seconds,1 minute and 5 minutes. For the radio data we have used flux data from IPS database [9]. The data was recorded by Learmonth Observatory,Western Australia. The data contains radiation flux data for 8 frequency:245 MHz, 410 MHz,610 MHz,1415 MHz,2695 MHz,4975 MHz,8800 MHz and 15400 MHz. The time step is 1 second. Since the observation is done from earth's surface the data is only available for an average 11 hours a day.

Chapter 2

Study of underlying Distributions of data

The existence of power law in radiation flux of astronomical bodies was proven long back and numerous studies have reported different values of Power law index[2][3].

2.1 Power law index

Any physical process is said to follow power law if the frequency distribution $f(x)$ of the indicator value x of that process has the relation,

$$\mathbf{f}(x) \sim x^p \tag{2.1}$$

where p is the power law index. The value of the power law index is one of the defining attributes of given process and its value can be used for identifying different stages of the process.Since frequency distribution can be converted to probability distribution by normalizing, the power law index can be used to calculate the probability of the system to be in a given state.

From the previous graph we can see that power law index does not possess a single value but varies in accordance with the solar cycle. The intensity distributions for 1989,1990 and 1991 shows how the distribution changes with the solar cycle as the whole distribution moves towards the high intensity region for 1990 and starts reverting in 1991. This change is also observed in the power law index for these years.

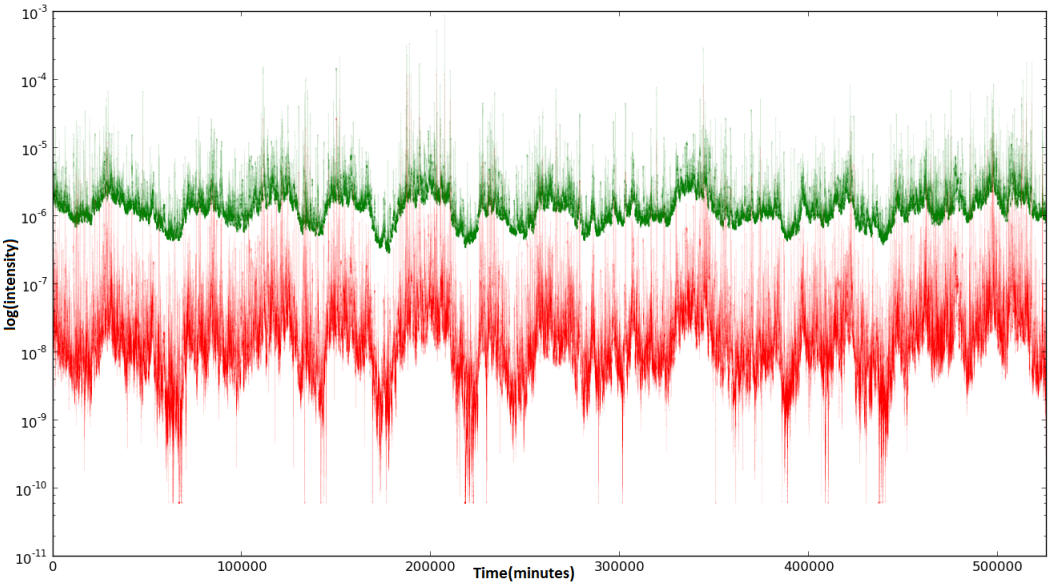

Figure 2.1: **log(Intensity) verses time(min)**. The top line pertains to X-ray long channel and bottom to short channel.This graph shows how the actual data set looks like.

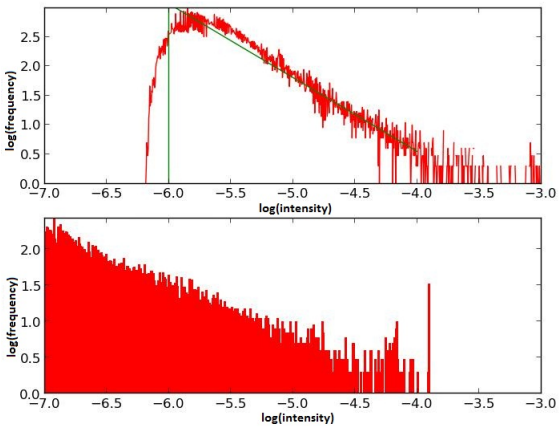

Figure 2.2: **Intensity distribution** .intensity distribution on log scale of X-ray long channel(above) $p = 1.29$ and short channel(below) for 1989.

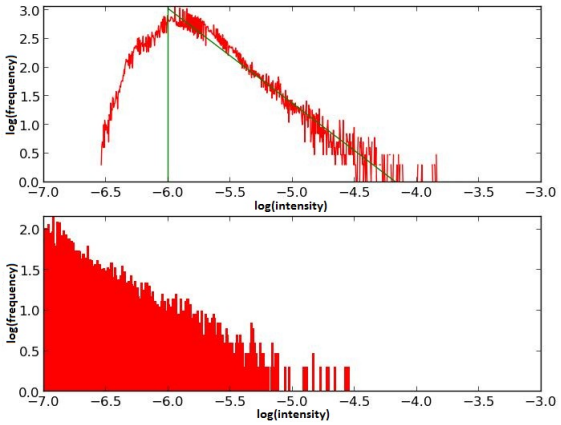

Figure 2.3: **Intensity distribution** .intensity distribution on log scale of X-ray long channel(above) $p = 1.75$ and short channel(below) for 1990.

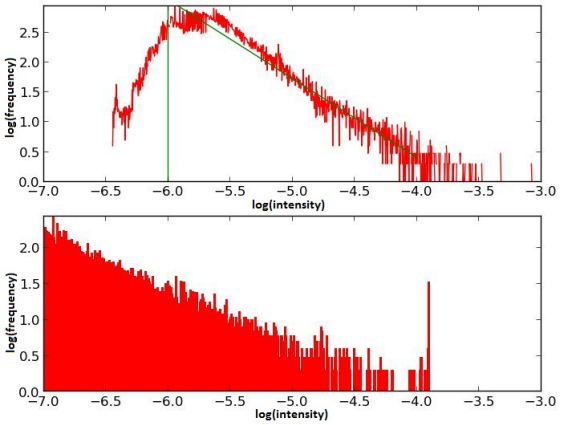

Figure 2.4: **Intensity distribution** .intensity distribution on log scale of X-ray long channel(above) $p = 1.36$ and short channel(below) for 1991.

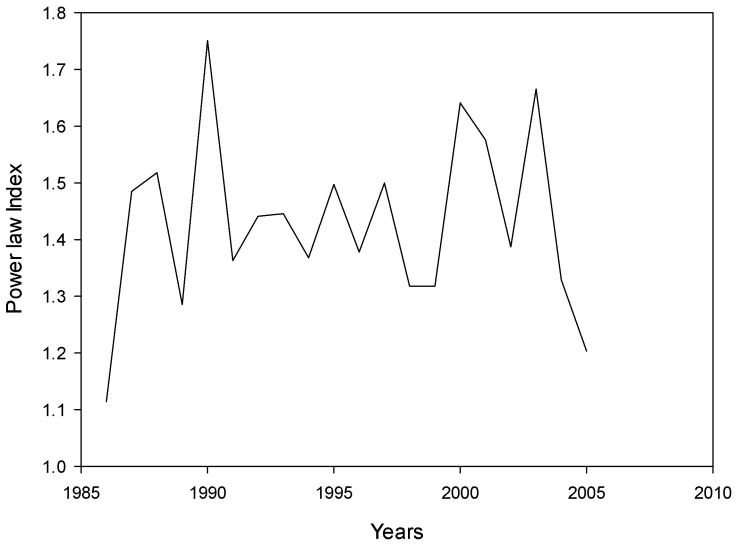

Figure 2.5: **Power law index as function of years**.

2.2 Waiting Time Distribution

Waiting time is defined as duration after which the system passes a given threshold. For our purpose the threshold we chose was C-class solar flares and above which corresponds to intensities above $10^{-7}W/m^2$. For all classes greater than C-class in magnitude doesn't have enough events for a distribution. The range of power law index for waiting time distribution for C-class flares and above is 1.4-3.4 for different phases of solar cycle. These values are similar to the values mentioned in [1].These years were chosen such that both minimum and maximum phase of solar cycle are covered and there is an overlap between the data sets used here(1986-2010) and [1](1975-2001).

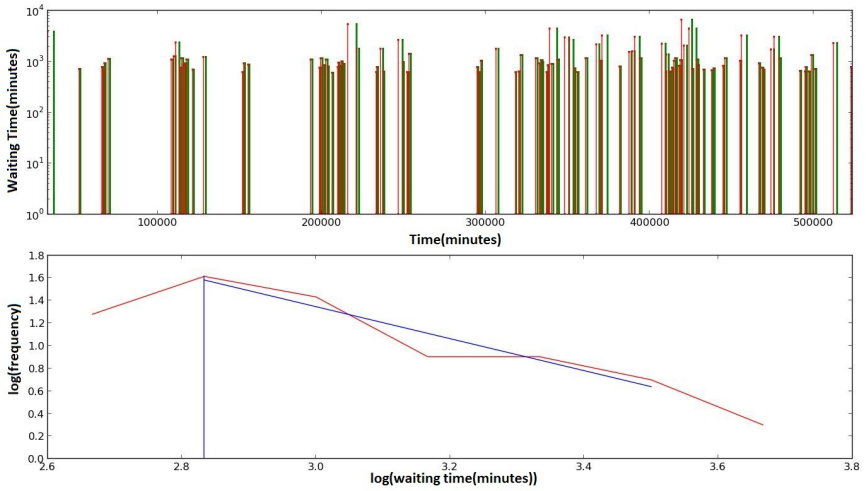

Figure 2.6: **Waiting-time distribution 1987**. (a) Above graph shows time stamp(min) for waiting time with bar height showing the waiting time . (b) Below graph shows the distribution of waiting times.Slope of the line is 1.6 .

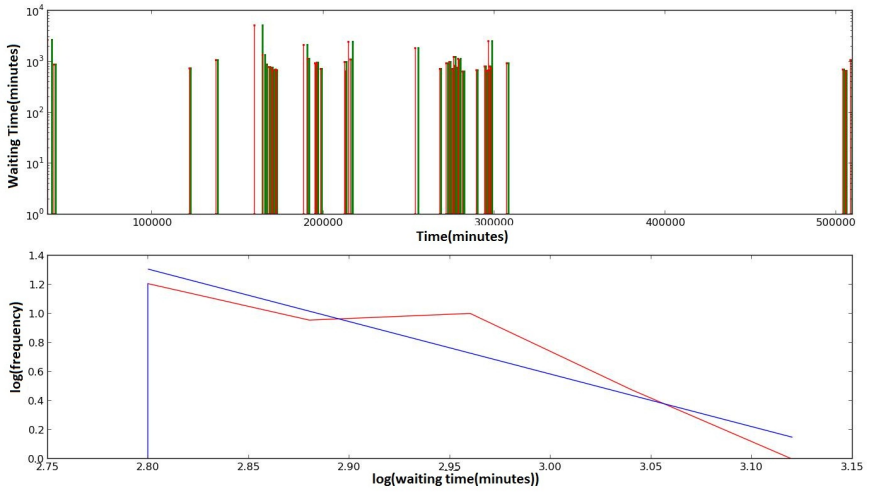

Figure 2.7: **Waiting-time distribution 1989**. (a) Above graph shows time stamp(min) for waiting time with bar height showing the waiting time . (b) Below graph shows the distribution of waiting times.Slope of the line is 1.4 .

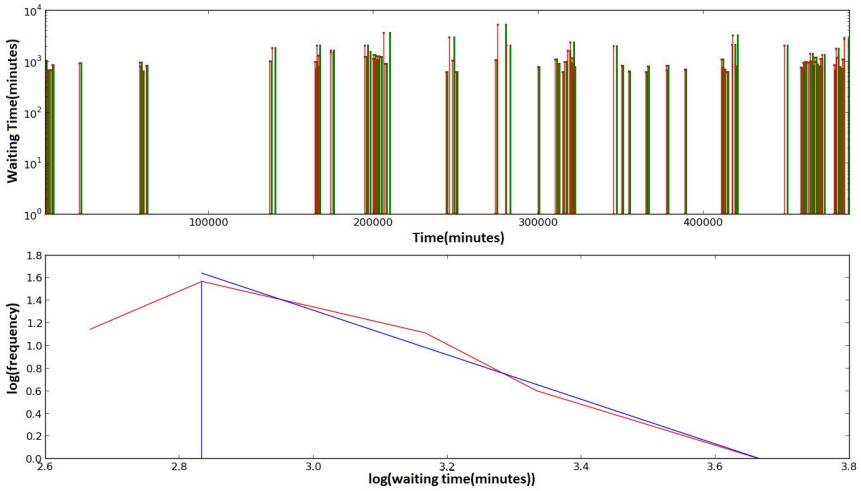

Figure 2.8: **Waiting-time distribution 1991**. (a) Above graph shows time stamp(min) for waiting times with bar height showing the waiting time . (b) Below graph shows the distribution of waiting times.Slope of the line is 3.4 .

Chapter 3

First difference of the time series

The first difference of the time series is the difference between intensities of consecutive time steps. For this study we took first difference recursively over same data set. The first difference represents the actual fluctuations in the data but each recursion results in loss of data points. Taking first difference recursively is similar to recursively taking differential of the same function. By analysing multiple levels of first difference we should be able to understand the overall process generating the time series.

3.1 Frequency Distribution of first differences

We calculated frequency distribution of first differences for each year of the available data and also for multiple years stacked together. We used long channel X-ray flux for first differences. The first difference is symmetrical for positive and negative first differences as seen in figure 3.1 which shows first difference as a function of time and also retaining the sign of the value. Figure 3.2 shows the same dataset with application of sign after taking log of the magnitude. Because of this symmetry we can use the absolute value of first difference for further analysis.

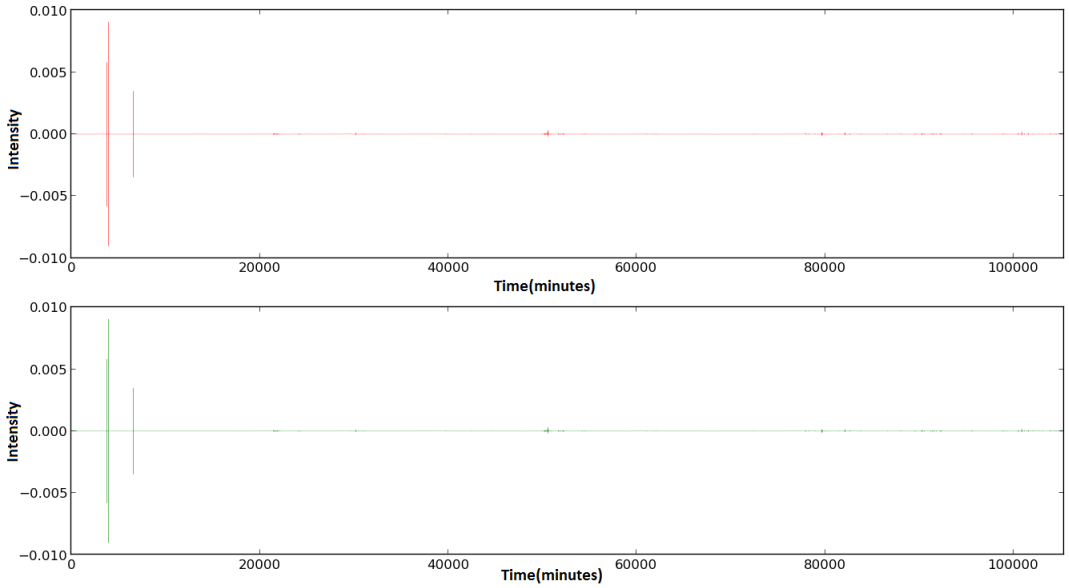

Figure 3.1: **First Difference 1988**. Time series of first difference of X-ray long channel for the year 1988.

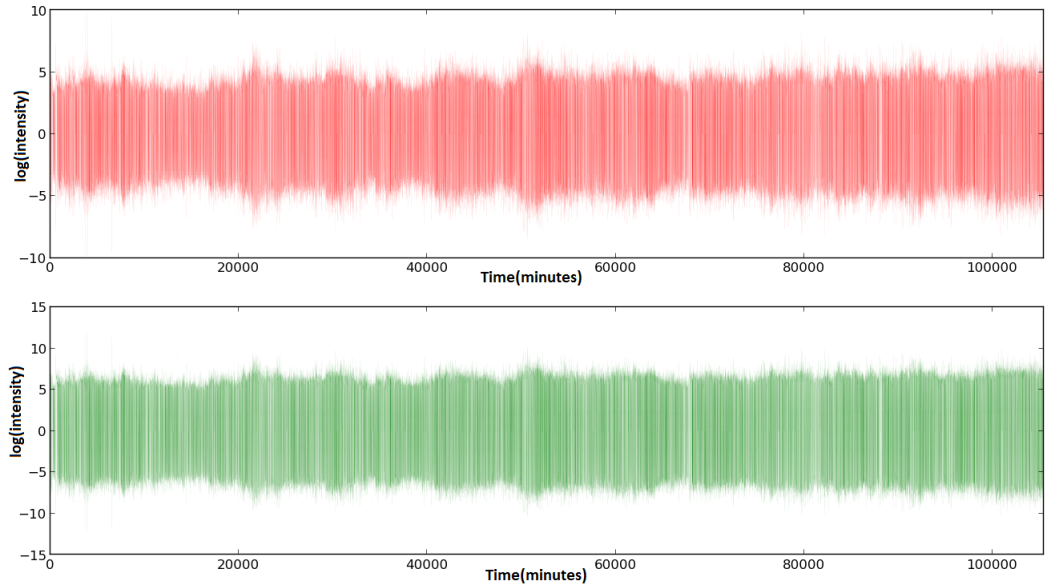

Figure 3.2: **First Difference 1988**. Time series of first difference of X-ray long channel for the year 1988 with y-axis in log scale.

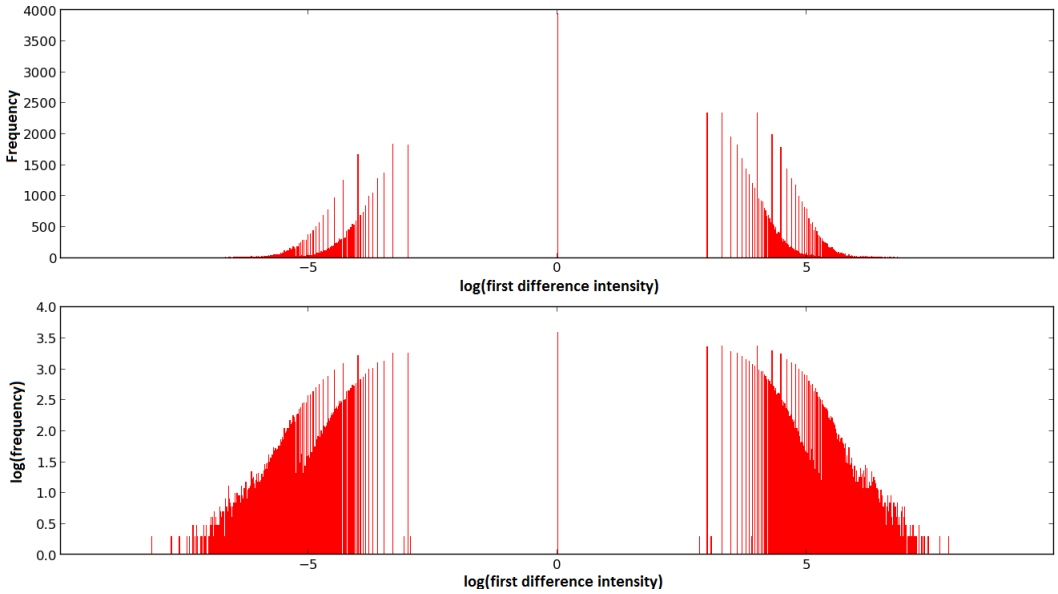

Figure 3.3: **Frequency distribution for 1988**.Frequency distribution of first difference of 1988 in log scale.

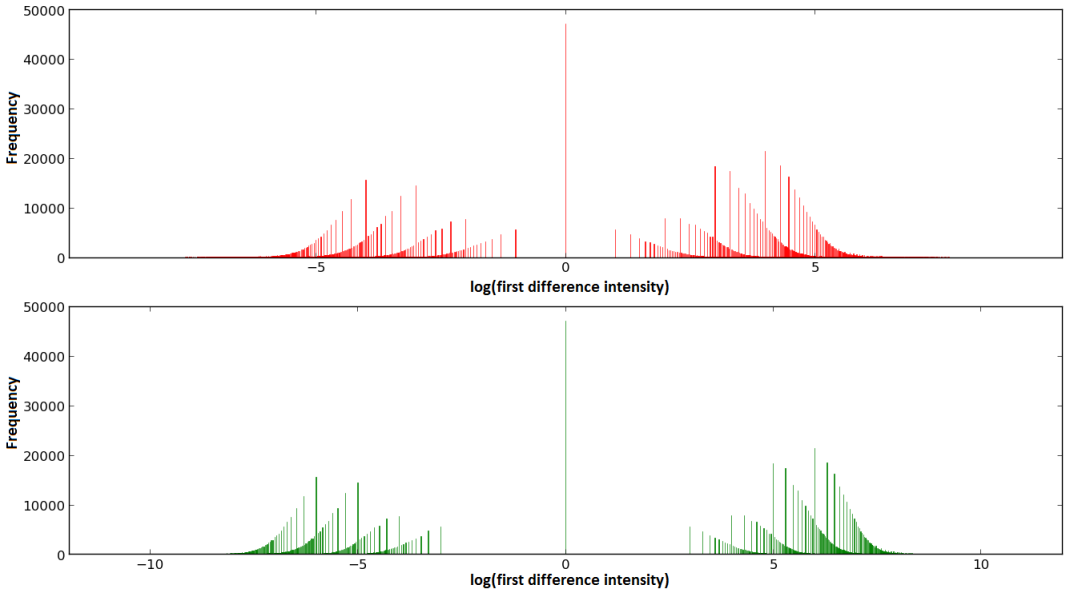

Figure 3.4: **Frequency distribution for 11 years**.Frequency distribution of first difference from 1987 to 1997 in log scale.

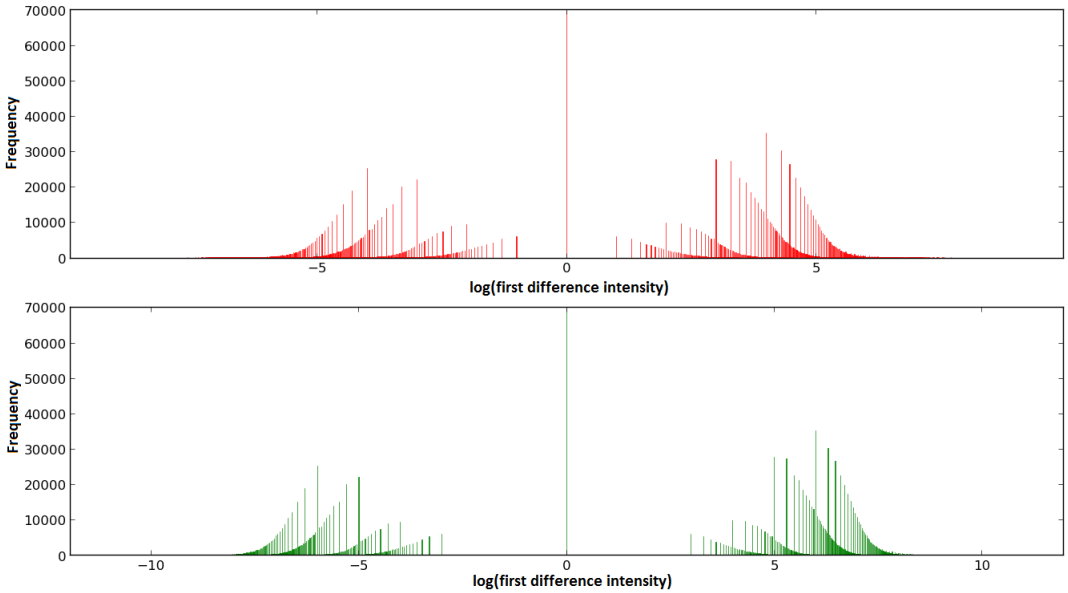

Figure 3.5: **Frequency distribution for 17 years**.Frequency distribution of first difference from 1986 to 2002 in log scale.

3.1.1 Note on frequency distribution of First differences

From the above graphs we can conclude that a unique pattern exists within the distribution of first differences. This pattern is invariant over time and also over different phases of solar cycle.At least a part of the distribution follows power law as is evident from the following graphs.

3.1.2 Note on Power law index of of First differences

We have calculated the power law index for the year 1988 for the original time series as well as for the series generated by taking first difference recursively three times. The power law index drops from 1.5 to 1.2 for first difference and then drops to 1 for next first difference and then remains stable at that value.

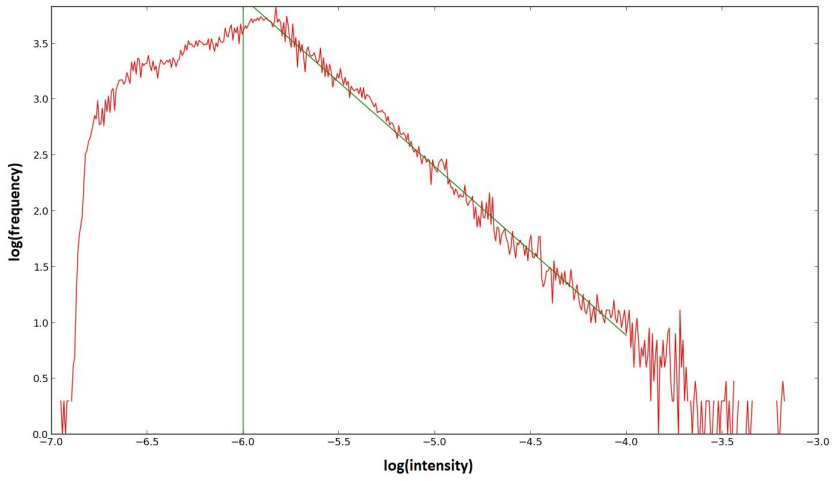

Figure 3.6: **Frequency distribution on log scale**. Original time series for the year 1988.Power law index is 1.5 .

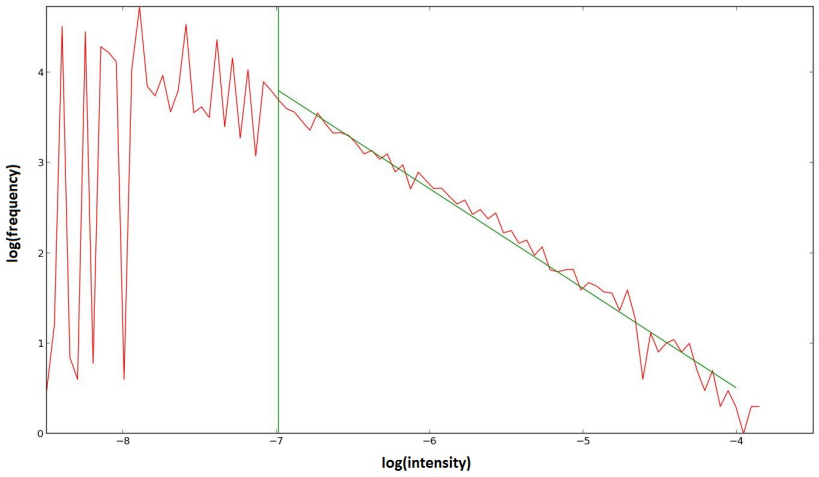

Figure 3.7: **Frequency distribution on log scale**. First difference for the year 1988.Power law index is 1.2 .

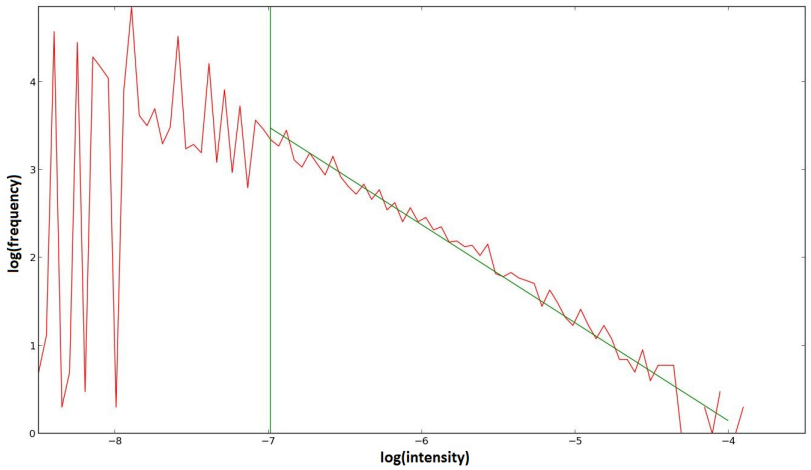

Figure 3.8: **Frequency distribution on log scale**. First difference of first difference for the year 1988.Power law index is 1.0 .

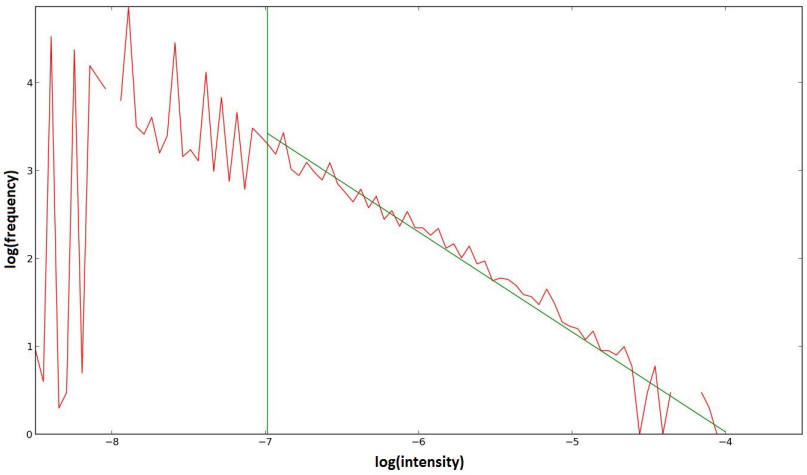

Figure 3.9: **Frequency distribution on log scale**. First difference of first difference of first difference for the year 1988.Power law index is 1.0 .

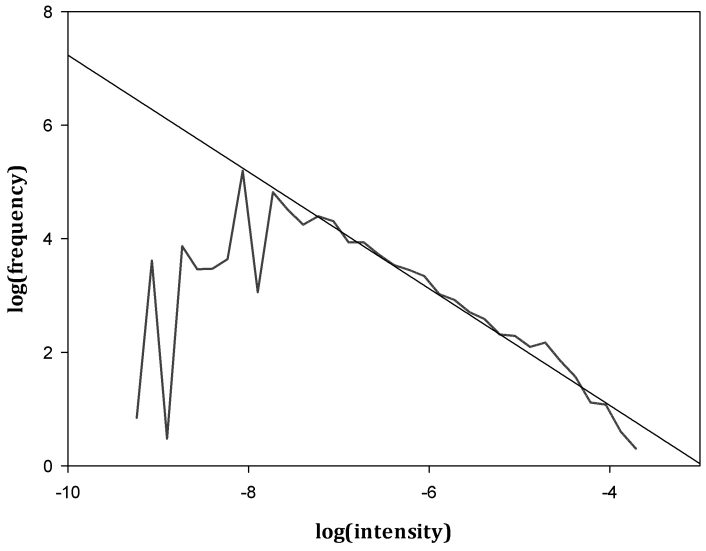

Figure 3.10: **Frequency distribution on log scale**. First difference of first difference of first difference for the year 1989.Power law index is 1.01 .

The changes in power law index from the original time series(fig 3.6) to its first difference (fig 3.7) indicates that the first difference is more evenly distributed(magnitude of intensity) than the original series which follows for the next first difference(fig. 3.8) also. But when we take the first difference one more time the power law index remains the same(fig 3.9). Fig. 3.10 shows dataset at same level as fig. 3.9 but for the year 1989.The power law index for 1989 for the original series is 1.29(fig. 2.2). From here we see that the power law index changes for the original time series for the two years(1988 and 1989) but after taking first differences 3 times the resultant dataset has same power law index. This can be interpreted in two ways:

1 The effect of solar cycle diminishes at this level. This also means that the solar x-ray flux is controlled by atleast two separate processes. One controlling the base flux and one generating the solar cycle.

2 The solar cycle is a result of different datasets generated from same fluctuation data. Since the distribution of the base fluctuation doesn't change,the different flux levels at different periods of solar cycle must be generated through different combinations of base fluctuations.

Chapter 4

Fluctuation analysis

To further analyse the fluctuation in the data we calculated DFA(Detrended Fluctuation Analysis) exponent for our data sets. This also gave us an overview of correlation and its length within the time series. Since we have a non-stationary time series calculating autocorrelation directly is quite difficult.

4.1 DFA

Detrended Fluctuation Analysis is an analysis method that reduces the effects of scaling within the data due to non-stationary mean.

For a time series $x_i(i = 1..N)$ we calculate,

$$\mathbf{y}(i) = \sum_{j=1}^{N} [x_j - \langle x \rangle] \tag{4.1}$$

where $\langle x \rangle$ is the mean of the time series. Next, $y(i)$ is partitioned into n boxes. Each box is fitted with a local trend $y_n(i)$. Subtracting $y_n(i)$ from $y(i)$ gives us the detrended time series $Y_n(i)$.

$$\mathbf{Y}_n(i) = y(i) - y_n(i) \tag{4.2}$$

Next we calculate the rms fluctuation $F(n)$,

$$\mathbf{F}(n) = \sqrt{\sum_{j=1}^{N} [Y_n(i)^2]/N} \tag{4.3}$$

For time series with power law correlations,

$$\mathbf{F}(n) \sim n^{\alpha} \tag{4.4}$$

where α is the DFA exponent or scaling exponent. For $\alpha = 0.5$ the time series is uncorrelated (white noise),$\alpha > 0.5$ the time series has long range correlation, $\alpha < 0.5$ the time series has short range correlation and $\alpha = 1$ the time series has infinite correlation length(1/f noise).

4.1.1 Note on DFA exponents

The following graphs show the DFA exponent for the original series and the corresponding first differences. There are several conclusions we can draw from this:

1 The DFA exponent for the original time series revolves around 1.0 which means the correlation length for the original time series is infinite.

2 The DFA exponent has an exponential decay as we recursively take first difference and calculate DFA for the new series. This seen from figure 4.2 which shows different levels of first difference along with boxes for 90 and 75 percentile of the median value. This is to show the number of outliers from the trend which comes out to be very few(2-3 in 62).

3 The DFA exponents for the the first differences along with the original series vary in different amounts but exhibit similar pattern. Figure 4.3 shows the trend for dfa exponent for different satellites over the years. Since dfa exponent can be used as a measure for correlation within the data, it can safely assumed that the correlation length for the original series and the first differences also follow the same trend.

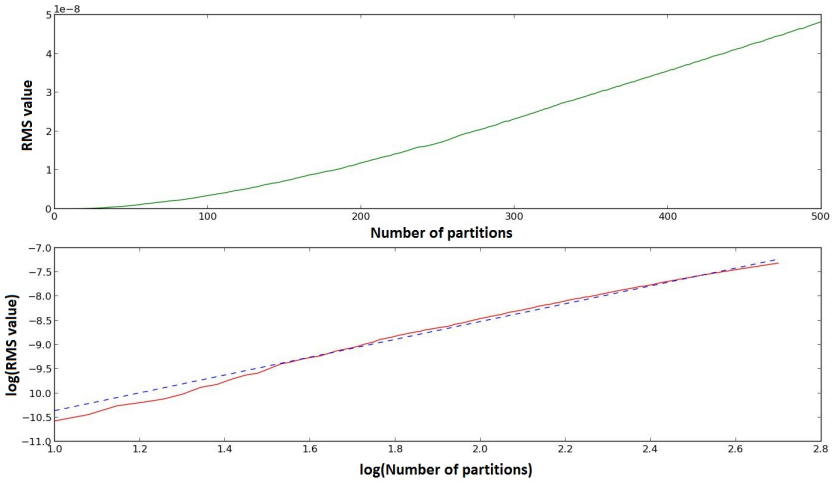

Figure 4.1: **RMS function for year 1998**. The slope of the above graph gives the dfa exponent for that data set.In this case it is 1.08

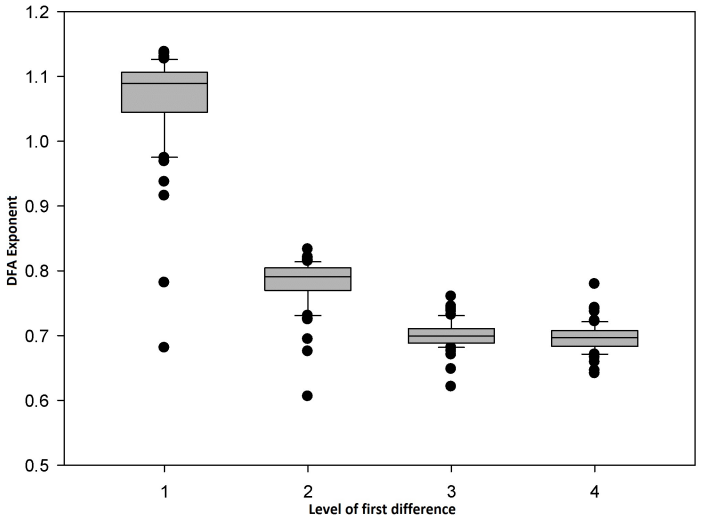

Figure 4.2: **DFA exponents with median values**. The data set is same as previous graph with each vertical set of points from left to right corresponding to the order in previous graph top to bottom.The boxes corresponds to 75 and 90 percentile of median.

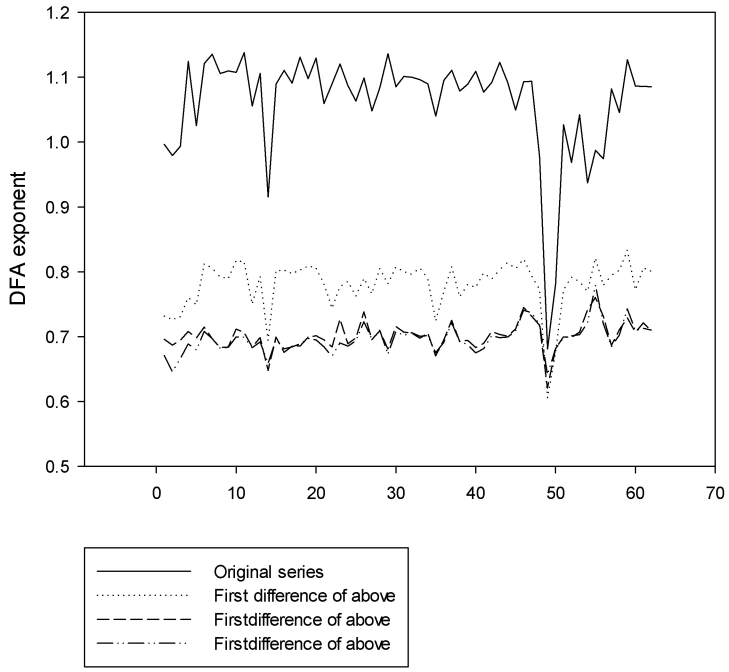

Figure 4.3: **DFA exponents**. DFA exponents for years 1986 to 2010 for all operational GOES satellite during that period.Note: X-axis is just index.The exponents were first sorted satellite wise and then year wise and then indexed over.Index 01-03 for GOES05,04-13 for GOES06,14-24 for GOES07,25-34 for GOES08,35-38 for GOES09,39-51 for GOES10,52-56 for GOES11 and 57-62 for GOES12

Chapter 5

Discussion

We started by analysing original series and calculating the power law indexes. Previously, the power law index for solar radiation flux has been treated as a constant and stating the fluctuations as deviation from the standard value but in our result we saw that not only the fluctuations are large they depend on the solar cycle and vary accordingly.

We didn't see any difference in waiting time distribution from the previously reported result. By recursively taking first difference we observed that the underlying structure of the radiation flux also follows power law and has long range correlation. Also after three levels of recursively calculating first difference the power law index stabilizes. The existence of 1/f noise in the original time series proves that all prediction systems depending on sample data set can never completely predict solar radiation flux as the one mentioned in [2]. But same can be applied to first difference as both follow power law and moreover first differences have finite correlation length and less fluctuation in the data.

References

[1] M. S. WHEATLAND and Y. E. LITVINENKO, UNDERSTANDING SOLAR FLARE WAITING-TIME DISTRIBUTIONS, Solar Physics(2002), **211**, 255-274.

[2] M. S. Wheatland, A Statistical Solar Flare Forecast Method, SPACE WEATHER Vol. 3, No. 7, S07003 , DOI:10.1029/2004SW000131(2005) .

[3] Gelu M. Nita, Dale E. Gary, L. J. Lanzerotti, and D. J. Thomson, THE PEAK FLUX DISTRIBUTION OF SOLAR RADIO BURSTS, The Astrophysical Journal (2002), **570**, 423-438.

[4] Kun Hu, Plamen Ch. Ivanov, Zhi Chen, Pedro Carpena, and H. Eugene Stanley Effect of trends on detrended fluctuation analysis, PHYSICAL REVIEW E, VOLUME 64, 011114.

[5] Jan W. Kantelhardt, Eva Koscielny-Bunde, Henio H. A. Rego, Shlomo Havlin, and Armin Bunde, Detecting Long-range Correlations with Detrended Fluctuation Analysis, Physica A 295 (2001), 441.

[6] Markus J. Aschwanden and Samuel L. Freeland, Automated Solar Flare Statistics in Soft X-rays over 37 Years of GOES Observations - The Invariance of Self-Organized Criticality during Three Solar Cycles, The Astrophysical Journal 754 (2012), 112.

[7] Website for data access for Solar X-ray flux: `http://satdat.ngdc.noaa.gov/sem/goes/data/avg/`.

[8] Website for information on satellites and other related resources: `http://www.ngdc.noaa.gov/stp/satellite/goes/dataaccess.html`.

[9] Website for data access for Solar Radio flux: `http://www.ips.gov.au/World_Data_Centre/1/10`.